Encapsulation in Charged Droplets Generates Distorted Host-Guest Complexes

Daniel L. Stares[a], Agnieszka Szumna*[b], and Christoph A. Schalley*[a]

Dedicated to Wei Jiang. May he rest in peace.

[a] D. L. Stares, Prof. Dr. C. A Schalley
Institut für Chemie und Biochemie, Freie Universität Berlin
Arnimallee 20, 14195 Berlin (Germany)
E-mail: c.schalley@fu-berlin.de
[b] Prof. A. Szumna
Institute of Organic Chemistry, Polish Academy of Sciences
Kasprzaka 44/52, Warsaw (Poland)
E-mail: agnieszka.szumna@icho.edu.pl

Supporting information for this article is given via a link at the end of the document.

Abstract: The ability of various hydrogen-bonded resorcinarene-based capsules to bind α,ω-alkylbisDABCOnium (**DnD**) guests of different lengths was investigated in solution and in the gas phase. While no host-guest interactions were detected in solution, encapsulation could be achieved in the charged droplets formed during electrospray ionisation (ESI). This included guests which are far too long in their most stable conformation to fit inside the cavity of the capsules. A combination of three mass spectrometric techniques, collision-induced dissociation, hydrogen/deuterium exchange, and ion-mobility mass spectrometry together with computational modelling allow us to determine the binding mode of the **DnD** guests inside the cavity of the capsules. Significant distortions of the guest into horseshoe-like arrangements are required to optimise cation-π interactions with the host which also adopt distorted geometries with partially open hydrogen-bonding seams when binding longer guests. Such quasi "spring-loaded" capsules can form in the charged droplets during the ESI process as there is no competition between guest encapsulation and ion pair formation with the counterions that preclude encapsulation in solution. The encapsulation complexes are sufficiently stable in the gas phase – even when strained – because non-covalent interactions significantly strengthen in the absence of solvent.

Introduction

Electrospray ionisation (ESI) is the most common methods of generating gaseous ions as it is soft and proceeds directly from solution.[1] ESI has been shown to be capable of accelerating reaction rates,[2] facilitating the self-assembly of supramolecular systems[3] and is even able to form complexes which cannot be observed in solution;[4] a prominent example of this being the serine octamer clusters.[5] An interesting aspect of ESI is that the transient charged droplets which form offer an environment where charge neutrality is violated enabling novel chemistry to occur. This can potentially be useful for host-guest complexes binding charged guests as counterion(s) will be stripped away obviating any ion pairing issues that may be present in solution and enables direct interaction of the naked ion with the host aiding binding. Because of this, it is possible to generate unusual host-guest complexes and binding modes not observed in solution, which then survive transfer into the gas-phase due to the strengthening of most non-covalent interactions in the absence of solvent.[6]

To study the unique complexes which form in these charged droplets, it is necessary to utilise mass spectrometry (MS). As mass-to-charge ratio (*m/z*) alone does not provide details on an ion's structure, more advanced MS techniques are required to investigate the ions such as collision-induced dissociation (CID), gas-phase hydrogen deuterium exchange (HDX), ion-mobility mass spectrometry (IMS). With these techniques, it is possible to elucidate structural and energetic information of an ion and thus gain insight into the chemistry occurring in the charged droplets.

Resorcinarenes are widely used hosts which can bind cations thanks to an electron-rich bowl-shaped cavity.[7] Resorcinarenes can self-assemble into dimeric[8] and hexameric capsules[9] and offer great versatility owing to potential modifications of both their upper and lower rims, forming diverse hydrogen-bonded,[10] metallo-supramolecular,[11] anion-based,[12] and halogen-bonded capsules.[13] Such modular design allows for the modification of cavity size and function potentially encapsulating a range of guests both in terms of size[14] and class of guest, with even anion binding being possible with the appropriate modifications.[15]

Herein, we report the encapsulation of different length dicationic α,ω-alkylbisDABCOnium (**DnD**) guests into hydrogen-bonded resorcinarene-based capsules. No interaction was seen in solution, but encapsulation could be promoted via ESI including guests which should be too long to fit inside the cavity. In these cases, encapsulation requires large distortions of the host-guest complexes which could be uncovered by a combination of MS and computational modelling. The encapsulation of these guests is a prototypical example of chemistry occurring under conditions violating electroneutrality, forming complexes not observed in solution. This offers qualitative insight into the enhanced non-covalent interactions in the absence of solvent and highlights the three very different environments that the complexes encounter:

solution, charged droplets and the gas phase.

Results and Discussion

The cavitands are synthesised by acylhydrazone linkage of a hydrazide containing strand to a tetraformylated resorcinarene precursor (Scheme 1). Previously, cavitands capable of dimerising via N-H···O hydrogen bonds were prepared by attaching mono-, di-, tri- and tetrapeptide strands to the upper rim of resorcinarenes.[16] It was expected that the longer strands would result in larger cavities when dimerising, however, cavity size did not change as the capsules were only engaging the first amino acid for intermolecular hydrogen bonding leaving the terminal ends of the strands unbound.

In the current study, the strand was shortened to an acetyl moiety which resulted in the formation of a new hydrogen-bonded dimer of this type (**1**) (Figure 1a). Dimer formation of **1** was supported by both Diffusion-Ordered Spectroscopy (DOSY) and Rotating Frame Overhauser Enhancement Spectroscopy (ROESY) (Figures S3 & S4) and suggests a binding motif involving a continuous seam of eight hydrogen bonds propagating around the capsule (Figure 1a). Comparing models of **1_2** (Figure 1a) and the previously reported phenylalanine peptide capsule **2_2** (Figure 1b)[16a] shows that shortening the chain to an acetyl moiety reduces the dimensions and thus **1_2** and **2_2** can be used to monitor the effect of cavity size on guest binding. The guests used were DABCO heads connected by alkyl chains of different lengths (**DnD,** n = 2–12, Figure 1c) which should bind with the electron-rich resorcinarene cores via cation-π interactions because of the guest's double charge.[17] The double charge allows interaction with both hemispheres of **1_2** and **2_2** whilst Coulomb repulsion between the two charges should favour full extension of the **DnD** enabling an assessment of guest size on binding.

Because of the ring current within the four aromatic rings of the resorcinarene core, encapsulation of the guest into the capsule's cavity would produce clear upfield shifts of the guest's ^{1}H nuclear magnetic resonance (NMR) signals. NMR measurements for these compounds were hampered by solubility issues as **1_2** and the **DnD**·$(PF_6)_2$ salts were not soluble in the same solvent at the concentrations required for NMR. Solvent mixtures can be used, but this was complicated by the competitive nature of most polar solvents for hydrogen bonding meaning they can only be used in small amounts.[16] A 4:1 chloroform: acetonitrile mixture dissolved **1_2** and **D5D**·$(PF_6)_2$ however, no shifts that indicate encapsulation were observed (Figure S11).[18]

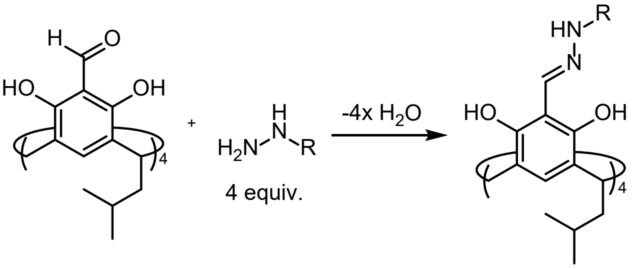

Scheme 1. Formation of the cavitands via acylhydrazone chemistry.[16]

The same result was obtained when guest salts with tetrakis[3,5-bis(trifluoromethyl)phenyl]borate (**BArF**) counterions were used.[19] **BArF** is less coordinating than PF_6^- and increases solubility in non-polar solvents such that **D9D**·(**BArF**)$_2$ and **1_2** were both soluble in pure dichloromethane. Still, no interaction between host and guest was observed (Figure S12). No changes were seen when samples were re-measured after several days (Figure S13), nor was interaction seen when measuring with different **DnD** guests (Figure S14). Thus, from the NMR analysis, it is clear that guest encapsulation does not occur in solution, even in non-competitive solvents such as dichloromethane.

In marked contrast, strong signals for ions corresponding to the dimer/guest complex ([M_2+**DnD**]$^{2+}$) were observed for all guests with both **1_2** and **2_2** (Figures S16&17) in their ESI mass spectra. As the complexes do not exist in solution before ionisation and we can safely rule out their formation in the gas phase after the ESI process, the only conclusion is that the encapsulation has occurred in the positively charged droplets *during* ESI. In ESI, ions are formed via the desolvation of analyte ions in charged droplets (Figure S15).[20] These droplets contain an excess of positive charges from guests without counterions and thus, the effect of ion pair formation is waived allowing interactions between the naked cation and the capsule enabling encapsulation that cannot be seen in solution. Consequently, such encapsulation represents supramolecular chemistry occurring under conditions violating electroneutrality.

Although this clear-cut difference between NMR and MS results can be understood, some **DnD** should be too long to bind so it is still surprising to see interactions between **1_2** or **2_2** and *all* guests. A straightforward explanation would be that this is due to a non-specific interaction between host and guest occurring during ESI i.e the **DnD** guests are binding externally rather than truly being encapsulated. To investigate this, the disassembly of the ions was studied via collision-induced dissociation (CID) where ions are accelerated by an electric field and collided with a neutral buffer gas. This converts some of the ions' kinetic energy into internal energy eventually leading to ion fragmentation, if this

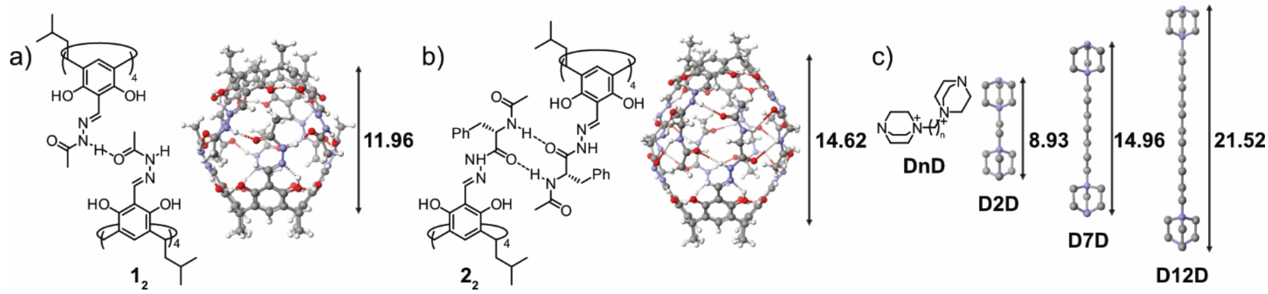

Figure 1. a) Acetylhydrazoneresorcinarene capsule (**1_2**); b) Phenylalanine resorcinarene capsule (**2_2**). The distances from lower rim to lower rim are marked in Å; c) **DnD** guests which should be fully extended due to charge repulsion. The $(CH_2)_3N$-$N(CH_2)_3$ distance shown (Å)

energy is sufficiently high (Figure 2a).[21] CID of the mass-selected $[\mathrm{M}_2+\mathbf{DnD}]^{2+}$ ions resulted in the loss of one cavitand unit to the $[\mathrm{M}+\mathbf{DnD}]^{2+}$ ion before further dissociation of the guest (Figures 2b,c). The intact free guest was not observed for the shorter chain length guests ($n \leq 3$) due to the strong repulsion of the two charges over such short range in the gas phase (Figure S18),[22] but the initial cavitand loss was seen for all guests and hosts. This dissociation pathway already supports the hypothesis of guest encapsulation over non-specific binding as guest loss would certainly dominate, if the guest was non-specifically bound to the outer surface of the capsule. The relatively high collision voltage required to induce dissociation also speaks against non-specific binding as such interaction would only be weak and the non-specific complexes would thus dissociate at much lower collision voltages.[23] A relative ranking of gas-phase stabilities can be analysed by survival yield (SY) plots which can be constructed by calculating parent ion relative intensity at increasing collision voltages and plotting the two against each other.[24] This produces a sigmoidal curve where the inflection point represents the voltage at which the parent ion intensity is half of the total intensity ($\mathrm{SY}_{50\%}$), with higher $\mathrm{SY}_{50\%}$ values indicating greater stability (Figure S20). For $[\mathbf{1}_2\subset\mathbf{DnD}]^{2+}$, a similar stability is observed for n = 2–5 followed by a gradual and consistent decrease in $\mathrm{SY}_{50\%}$ values at longer chain lengths (Figure 3d). The same trend was also observed for $\mathbf{2}_2$, but the stability decreases from n = 7 (Figure S21), reflecting the larger cavity of $\mathbf{2}_2$ compared to $\mathbf{1}_2$.

The CID results indicate guest encapsulation even for those **DnD** longer than the cavity size. A possible explanation for the encapsulation of these guests is a rupturing of the intermolecular hydrogen bonding between the cavitands with the guest bridging the two partially or completely separated monomers (Figure 3a). To investigate this, measurements were performed with an N,N-dimethylhydrazone derivative (**3**) (Figure 3a) which cannot form intermolecular hydrogen bonds so can only dimerise via a bridging guest. In contrast to $\mathbf{1}_2$ and $\mathbf{2}_2$, $[\mathbf{3}_2+\mathbf{DnD}]^{2+}$ ions were only observed for $n \geq 5$ indicating that dimeric complexes with shorter guests are not very stable. SY analysis of $[\mathbf{3}_2+\mathbf{DnD}]^{2+}$ showed *increasing* stability with guest length until **D10D** where a plateau was reached (Figure 3b). This stability trend is expected for a complex in which no additional interactions between host cavitands exist where very short guests can only bridge the two monomers with destabilizing steric clashes between them. The steric clashes reduce with medium-sized guests permitting dimer formation, which becomes energetically more and more favourable with guest length until a threshold distance is reached where the two monomers are fully separated so that stability does not change anymore with longer guests. The fact that the inverse trend is observed for $\mathbf{3}_2$ suggests $\mathbf{1}_2$ and $\mathbf{2}_2$ are maintaining hydrogen bonding between the cavitands in some manner.

An explanation for encapsulation, while maintaining hydrogen bonding between the cavitands, would involve distortion of the guests from their fully extended form to fit inside the cavity. It has been demonstrated in solution that alkane guests can bind inside resorcinarene capsules by coiling into a helical arrangement.[25] If a similar coiling is occurring here, the SY trends where longer guests destabilize the capsule can be rationalised by the strain associated with deviation from the ideal guest geometry in addition to the increased charge repulsion at the shorter distance. Guest coiling can be monitored via gas-phase hydrogen/deuterium exchange (HDX) experiments and can be conducted with a Fourier-Transform Ion-Cyclotron-Resonance (FTICR) mass spectrometer, allowing for precise control of reaction intervals with both the number and rate of exchange(s) being structurally informative.[26] HDX will shift from a fast concerted, Grotthus-like mechanism, to a slower non-concerted process that involves unfavourable charge separation species

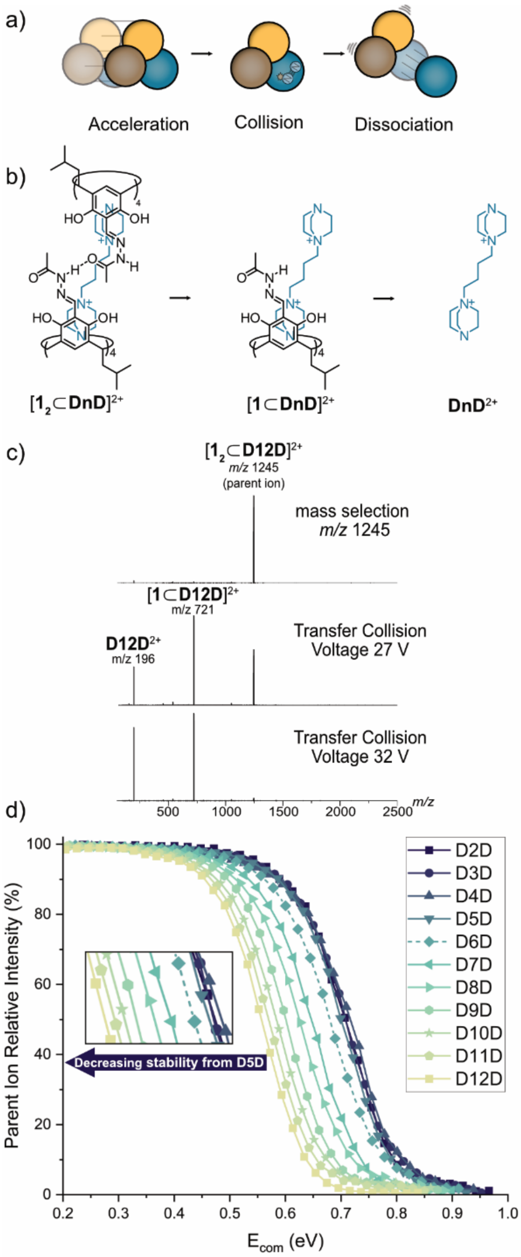

Figure 2. a) Principles of CID where the ions are accelerated into an inert collision gas converting kinetic energy into internal energy of the ion. Dissociation of the ion will follow if the internal energy is sufficiently high; b) Fragmentation pathway of $[\mathbf{1}_2\subset\mathbf{DnD}]^{2+}$ ion, which was seen for the other hosts and guests with $n \leq 3$; c) CID spectra for $[\mathbf{1}_2\subset\mathbf{D12D}]^{2+}$ d) SY curves of $[\mathbf{1}_2\subset\mathbf{DnD}]^{2+}$ with a zoom of the $\mathrm{SY}_{50\%}$ region show in the inset. Note that the collision voltage was converted to the centre of mass energy (E_{com}) as described in the supporting information.

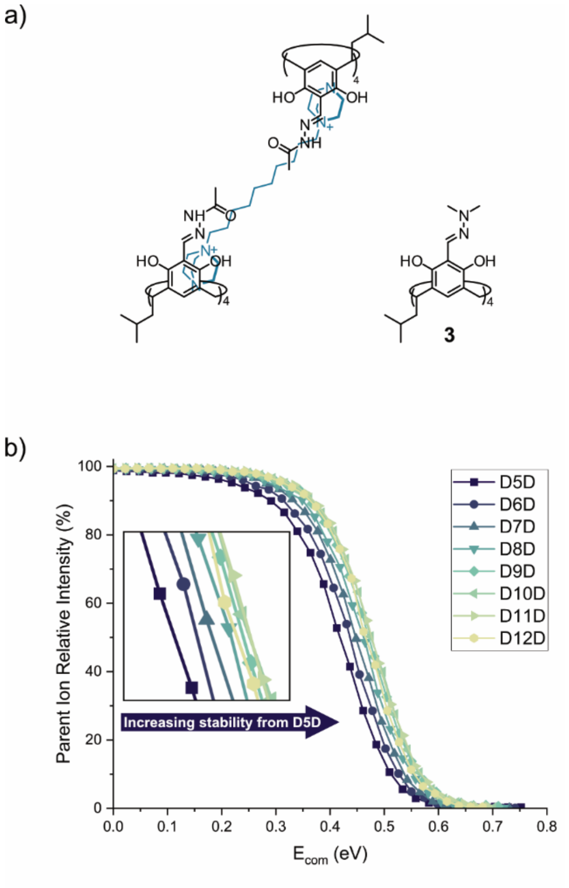

Figure 3. a) Non-hydrogen-bonded dimer where the **DnD** bridges across the two cavitands (left); N,N-dimethylhydrazoneresorcinarene (**3**) (right); b) SY curves of $[\mathbf{3}_2\mathbf{+DnD}]^{2+}$ with n = 5–12. A zoom of the SY$_{50\%}$ region of the curves is shown in the inset.

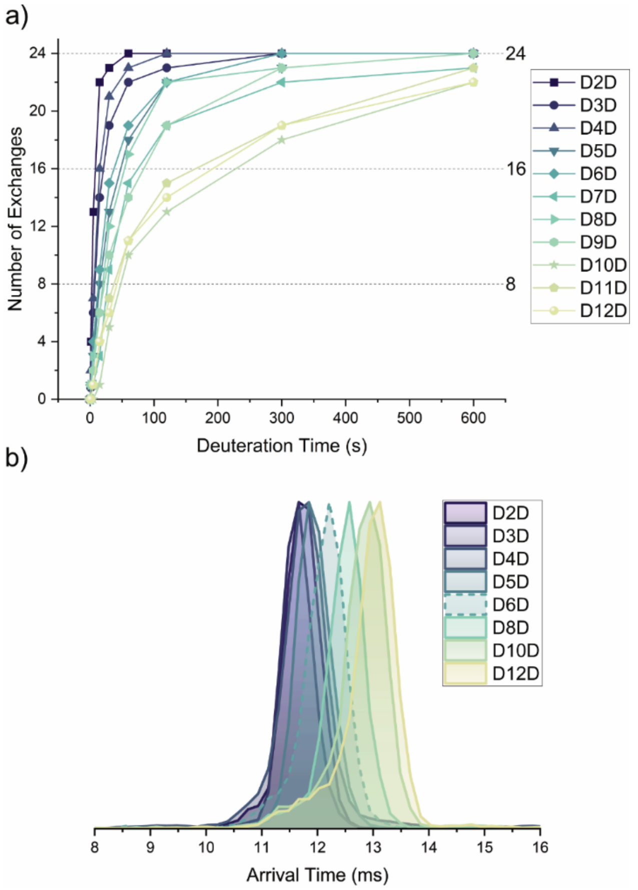

Figure 4. a) HDX for $[\mathbf{1}_2\subset\mathbf{DnD}]^{2+}$. The dashed lines represent the 8 NH and 16 OH which are exchangeable. The number of exchanges is consistent but the rate decreases for longer guests; b) ATDs of $[\mathbf{1}_2\subset\mathbf{DnD}]^{2+}$ for n =2-6,8,10,12 n=7,9,11 omitted for clarity

when a continuous hydrogen-bonding seam that runs around the capsule is disrupted (Figure S25).[27] The hydrogen bonding pattern of $\mathbf{1}_2$ would be expected to remain intact if the guests are coiling inside the cavity, and thus should produce similar HDX results with all guests. In the series of $[\mathbf{1}_2\subset\mathbf{DnD}]^{2+}$ ions, irrespective of the encapsulated guest, up to 24 exchanges were observed corresponding to the 8 N-H and 16 O-H hydrogens. However, the rate of exchange continually decreased from n = 5 onwards, correlating well to the CID results, and suggests guest binding modes which impact the N-H···O bonds between the strands. The HDX indicates smaller guests allow the capsule to form a fully closed, non-disrupted seam which results in fast exchange whilst for the intermediate-sized guests, the seam is opened occasionally due to steric clash with the guests reducing the exchange rate. The rate further slows with the longer guests as they have a constantly partially open seam preventing efficient exchange (Figure S21). These situations can be distinguished from each other with the orthogonal technique of IMS which provides structural information by determining the size of ions.[28] Simply speaking, IMS acts as a wind tunnel for ions by transmission of the ions through a cell filled with an inert drift gas. As the ions travel through this cell, they undergo low-energy collisions with the drift gas which decelerates the ions and hence a smaller ion that has fewer collisions will have a shorter drift time through this cell than a larger ion which undergoes more collisions. For host-guest systems, IMS can be used to infer conformational differences and guest binding modes.[29] When considering space-filling models of both $\mathbf{1}_2$ and $\mathbf{2}_2$ (Figure S27), they show an almost non-porous structure which would result in similar CCS of non-disrupted systems. Consequently, short guests which are encapsulated without disrupting the hydrogen bonding seam should all have comparable arrival times in IMS. Measurements of the $[\mathbf{1}_2\subset\mathbf{DnD}]^{2+}$ ions show similar arrival times for n ≤ 5 with gradual increases in drift time beyond this guest length (Figure 4b). These results, like HDX, also support the idea of a completely intact hydrogen bonding seam for the shorter guests which is then disrupted by the medium to long guests increasing drift times. Comparable IMS results were also obtained for $\mathbf{2}_2$ (Figure S22), but again shifted to the next larger guest in the series, consistent with the larger cavity. For **3**, a size increase was apparent for all guests with only slight increases seen for longer guests (Figure S23). In all cases, there is good agreement between the onset of size increase seen in IMS with the decreases in stability seen via CID.

The experimental results all correlate well to one another providing a consistent picture for all hosts. Computational modelling was then used to further explore the complexes. Such large systems make full DFT calculation computationally expensive, so final structures were optimised with the ORCA software using the HF-3c level of theory.[30] HF-3c incorporates the D3 dispersion corrections and offers a nice balance between accuracy and cost while being suitable for analysis of host-guest systems.[31] The computational models of the different complexes provided structures and binding modes in line with all the observed results. As the charge on the guests is more localised on the inner nitrogens, maximum cation-π interactions can be achieved by pointing these nitrogens into the resorcinarene core. As **3** does not benefit from any interaction between cavitands, it can interact with the fully extended guests with no penalty resulting in acute angles between **D12D** and the upper rims of the resorcinarenes (Figure 5). Such an arrangement is not possible for the shorter **D5D** due to potential steric clashes of the two monomers forcing a head on arrangement with a larger binding angle. The angle between the guest and the second resorcinarene decreases with longer guests and this binding mode in addition to decreasing steric and Coulomb repulsion, can explain the stability trends seen via SY analysis (Figure 3b). The longer guest also accounts for the continual increase in drift time seen in IMS (Figure S24), with the size convergence representing the point where the two resorcinarenes are parallel and pseudo-encapsulating the guests.

In $\mathbf{1_2}$, the guests also maximise cation-π interactions by pointing the inner nitrogen towards the electron-rich resorcinarene core. The intermolecular N-H···O hydrogen bonds between the strands prevent the simple translation of the two resorcinarenes (as with **3**) so, to be able to maintain cation-π interactions, the two DABCOniums are effectively locked in position. As a consequence, the carbon chain of the guest is forced to loop into a horseshoe-like arrangement. When the loop gets larger, it pushes against the strands of the host leading to a gradual weakening and eventual breaking of the H-bonds. Such weakening was first apparent with **D5D** which begins to strain the hydrogen bonds but allows the resorcinarene to reposition so that cation-π bonding is enhanced. This can account for the similar stabilities of **D2D**–**D5D** as the interplay between the weakening H-bonding is compensated by stronger cation-π interactions. Beyond **D5D**, longer guests continue to expand out of the cavity with the remaining H-bonds on the capsule effectively acting as a hinge to allow the portal to increase further. This can account for the observed stability trend seen in the SY curves as the hydrogen bonding on the strands near the guest loop continues to weaken when the loop grows. This would also decrease the HDX rate as the exchange begins to require a rearrangement which becomes more extreme with longer guests. Furthermore, as the strand is pushed away and the guests begin to expand outside the cavity, the collisional cross section (CCS) of the ion increases which

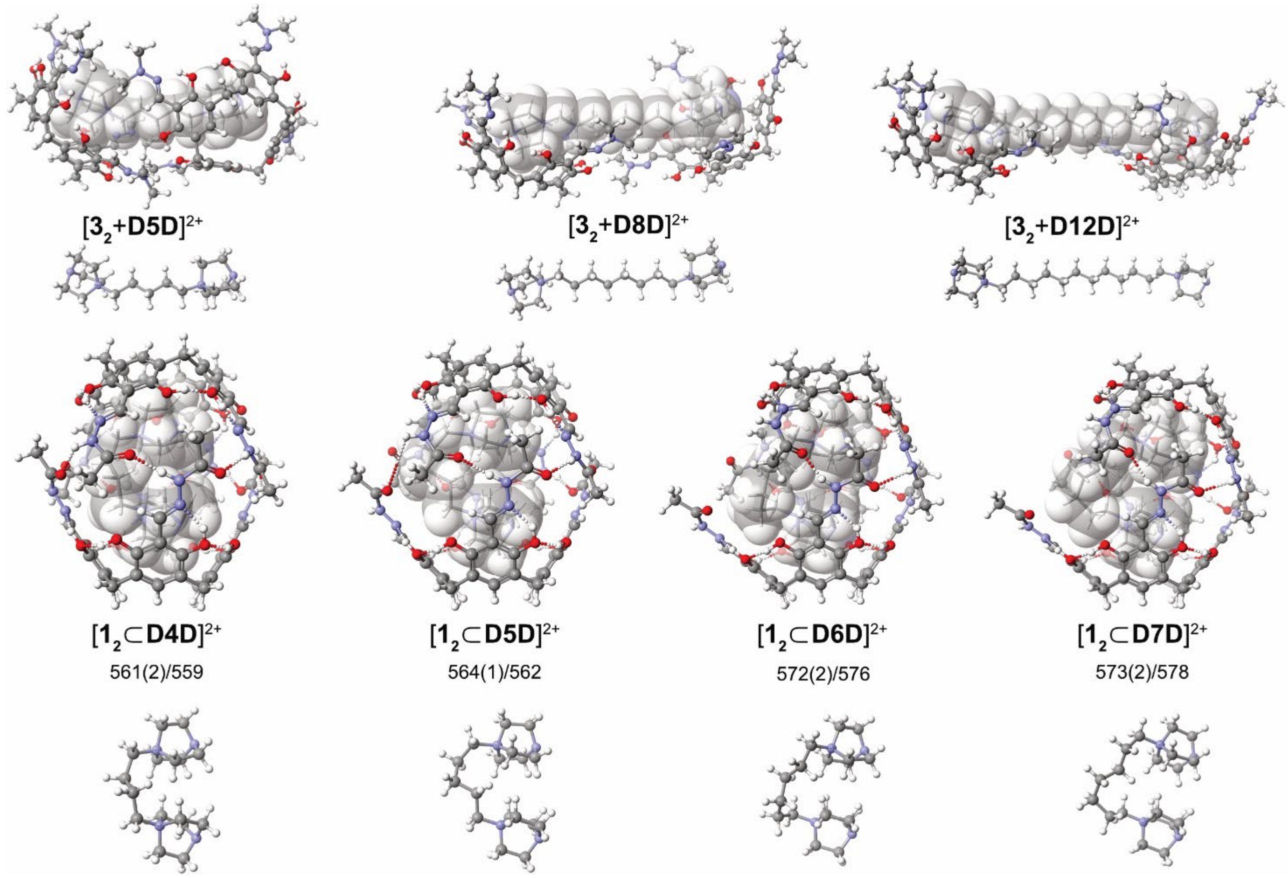

Figure 5. Computational structures of: $[\mathbf{3_2}+\mathbf{DnD}]^{2+}$ with n = 5, 8, 12 (top, left to right); $[\mathbf{1_2}\subset\mathbf{DnD}]^{2+}$ with n = 4, 5, 6, 7 (bottom, left to right), experimental ${}^{TW}CCS_{N2}$ values from CCS calibration (with standard deviation in parentheses) and theoretical ${}^{TM}CCS_{N2}$ values (as noted in the supplementary material) are given below the $[\mathbf{1_2}\subset\mathbf{DnD}]^{2+}$ structures. The bound guest is shown in space-filling mode and the encapsulated guest is shown without host underneath the respective host-guest structure. The bound guest geometry deviates greatly from that of the free guests. The *i-Bu* groups have been omitted for clarity.

contributes to the longer arrival time seen in IMS. IMS has the benefit of being able to link computationally generated model compounds to experimental results via the calculation of both experimental ($^{\mathrm{TW}}\mathrm{CCS}_{\mathrm{N2}}$) and theoretical collisional cross section values ($^{\mathrm{TM}}\mathrm{CCS}_{\mathrm{N2}}$) (Figure 5 & Table S3) which in this case have good agreement with one another.[32] Taken together, the theoretical and experimental results provide consistent results and strongly support the proposed binding mode of the **DnD** guests. These surprising binding modes represent a large deviation from the guest's preferred geometry (up to 16 Å, Table S4) against a Coulomb barrier and require rearrangement of the host to accommodate. Such a strained conformation persists in the gas-phase due to the strengthening of the non-covalent interactions that hold it together.

Conclusion

In conclusion, we have shown the ability of ESI to generate host-guest complexes which cannot be observed in solution. This is possible as the charged droplets formed during ESI offer an environment where ion pairing is obviated representing supramolecular chemistry occurring under conditions violating electroneutrality and reveals the intriguing chemistry that can result.

Using this strategy, guests too long for the cavity can be encapsulated in hydrogen-bonded resorcinarene capsules producing unusual conformations. The ion structures are assigned in the gas-phase with three structure-indicative MS techniques, CID, IMS and HDX which show decreasing stability above certain guest lengths and indicate guest expansion outside of the cavity for longer guests. The experimental results are coherent with one another and have been validated by computational modelling which reveals guest distortion into a horse-shoe arrangement upon encapsulation. This requires a large deviation of the guests from their ideal geometry in addition to distortions of the host, producing "spring-loaded" capsules with conformations that would be difficult to predict.

These complexes survive in the gas-phase, overcoming steric strain and the repulsion between the two DABCOnium moieties, due to the strengthening of the non-covalent interactions in the absence of solvent enabling investigation with MS. The ability of MS to unravel the conformation of these complexes is important as MS is uniquely positioned to study the chemistry occurring in these charged droplets.

We envisage that many unique binding motifs can be generated in this manner which can then be uncovered by MS.

Supporting Information

The authors have cited additional references within the Supporting Information. [16a, 19, 24a, 24b, 33]

Acknowledgements

We thank the European Union through the NOAH project (H2020-MSCA-ITN project Ref. 765297) and FU Berlin for funding. Support for measurements by the BioSupraMol core facility at FU Berlin is gratefully acknowledged. Fei Jia is acknowledged for providing some of the guests used for initial measurements. We are grateful to Janos Wasternack for the NaBArF salt and to Sebastian Müller for synthesising it and acknowledge the members of the Szumna group and IChO staff for their support during the secondment of DLS in Warsaw. Thank you to Marek Szymański for help with the synthesis of **2**.

Keywords: Mass Spectrometry • Host-Guest Chemistry • Resorcinarenes • Electrospray Ionisation • Charged droplets

[1] a) M. Wilm, *Mol. Cell. Proteomics* **2011**, *10*; b) P. Kebarle, L. Tang, *Anal. Chem.* **1993**, *65*, A972-A986; c) J. B. Fenn, *Angew. Chem. Int. Ed.* **2003**, *42*, 3871-3894; d) G. L. Glish, R. W. Vachet, *Nat. Rev. Drug Discov.* **2003**, *2*, 140-150.

[2] a) X. Yan, R. M. Bain, R. G. Cooks, *Angew. Chem. Int. Ed.* **2016**, *55*, 12960-12972; b) M. Girod, E. Moyano, D. I. Campbell, R. G. Cooks, *Chem. Sci.* **2011**, *2*, 501-510.

[3] N. K. Beyeh, M. Kogej, A. Åhman, K. Rissanen, C. A. Schalley, *Angew. Chem. Int. Ed.* **2006**, *45*, 5214-5218.

[4] a) J. Seo, S. Warnke, K. Pagel, M. T. Bowers, G. von Helden, *Nat. Chem.* **2017**, *9*, 1263-1268; b) S. Vandenbussche, G. Vandenbussche, J. Reisse, K. Bartik, *Eur. J. Org. Chem.* **2006**, *2006*, 3069-3073; c) D. P. Weimann, C. A. Schalley, *Supramol. Chem.* **2008**, *20*, 117-128.

[5] S. C. Nanita, R. G. Cooks, *Angew. Chem. Int. Ed.* **2006**, *45*, 554-569.

[6] L. Cera, C. A. Schalley, *Chem. Soc. Rev.* **2014**, *43*, 1800-1812.

[7] a) H.-J. Schneider, U. Schneider, *J. Incl. Phenomena Mol. Rec.* **1994**, *19*, 67-83; b) K. Kobayashi, M. Yamanaka, *Chem. Soc. Rev.* **2015**, *44*, 449-466.

[8] K. N. Rose, L. J. Barbour, G. W. Orr, J. L. Atwood, *Chem. Commun.* **1998**, 407-408.

[9] a) C. Gaeta, C. Talotta, M. De Rosa, P. La Manna, A. Soriente, P. Neri, *Chem. Eur. J.* **2019**, *25*, 4899-4913; b) M. Yamanaka, A. Shivanyuk, J. Rebek, Jr., *J. Am. Chem. Soc.* **2004**, *126*, 2939-2943; c) S. Gambaro, M. De Rosa, A. Soriente, C. Talotta, G. Floresta, A. Rescifina, C. Gaeta, P. Neri, *Org. Chem. Front.* **2019**, *6*, 2339-2347.

[10] a) T. Heinz, D. M. Rudkevich, J. Rebek, Jr., *Nature* **1998**, *394*, 764-766; b) H. Mansikkamäki, M. Nissinen, K. Rissanen, *Chem. Commun.* **2002**, 1902-1903.

[11] a) W.-Y. Pei, G. Xu, J. Yang, H. Wu, B. Chen, W. Zhou, J.-F. Ma, *J. Am. Chem. Soc.* **2017**, *139*, 7648-7656; b) R. Pinalli, V. Cristini, V. Sottili, S. Geremia, M. Campagnolo, A. Caneschi, E. Dalcanale, *J. Am. Chem. Soc.* **2004**, *126*, 6516-6517.

[12] a) M. Chwastek, P. Cmoch, A. Szumna, *Angew. Chem. Int. Ed.* **2021**, *60*, 4540-4544; b) M. Chwastek, P. Cmoch, A. Szumna, *J. Am. Chem. Soc.* **2022**, *144*, 5350-5358.

[13] a) N. K. Beyeh, F. Pan, K. Rissanen, *Angew. Chem. Int. Ed.* **2015**; b) O. Dumele, N. Trapp, F. Diederich, *Angew. Chem. Int. Ed.* **2015**, *54*, 12339-12344.

[14] a) D. Ajami, J. Rebek, Jr., *J. Am. Chem. Soc.* **2006**, *128*, 5314-5315; b) D. Ajami, J. Rebek, Jr., *Angew. Chem. Int. Ed.* **2007**, *46*, 9283-9286.

[15] S. S. Zhu, H. Staats, K. Brandhorst, J. Grunenberg, F. Gruppi, E. Dalcanale, A. Lützen, K. Rissanen, C. A. Schalley, *Angew. Chem. Int. Ed.* **2008**, *47*, 788-792.

[16] a) M. Szymański, M. Wierzbicki, M. Gilski, H. Jędrzejewska, M. Sztylko, P. Cmoch, A. Shkurenko, M. Jaskólski, A. Szumna, *Chem. Eur. J.* **2016**, *22*, 3148-3155; b) M. P. Szymański, J. S. Czajka, P. Cmoch, W. Iwanek, A. Szumna, *Supramol. Chem.* **2018**, *30*, 430-437.

[17] H. Mansikkamäki, C. A. Schalley, M. Nissinen, K. Rissanen, *New J. Chem.* **2005**, *29*, 116-127.

[18] R. J. Hooley, S. M. Biros, J. Rebek, Jr., *Chem. Commun.* **2006**, 509-510.

[19] B. Wüstenberg, A. Pfaltz, *Adv. Synth. Catal.* **2008**, *350*, 174-178.

[20] P. Kebarle, U. H. Verkerk, *Mass Spectrom. Rev.* **2009**, *28*, 898-917.

[21] a) L. Sleno, D. A. Volmer, *J. Mass Spectrom.* **2004**, *39*, 1091-1112; b) M. Rodgers, K. M. Ervin, P. B. Armentrout, *J. Chem. Phys.* **1997**, *106*, 4499-4508.

[22] C. A. Schalley, C. Verhaelen, F.-G. Klärner, U. Hahn, F. Vögtle, *Angew. Chem. Int. Ed.* **2005**, *44*, 477-480.

[23] T. Heravi, J. Shen, S. Johnson, M. C. Asplund, D. V. Dearden, *J. Phys. Chem. A* **2021**, *125*, 7803-7812.

[24] a) M. W. Forbes, D. A. Volmer, G. J. Francis, D. K. Böhme, *J. Am. Soc. Mass Spectrom.* **2005**, *16*, 779-791; b) T. M. Kertesz, L. H. Hall, D. W. Hill, D. F. Grant, *J. Am. Soc. Mass Spectrom.* **2009**, *20*, 1759-1767; c) N. Geue, T. S. Bennett, A.-A.-M. Arama, L. A. I. Ramakers, G. F. S. Whitehead, G. A. Timco, P. B. Armentrout, E. J. L. McInnes, N. A. Burton, R. E. P. Winpenny, P. E. Barran, *J. Am. Chem. Soc.* **2022**, *144*, 22528-22539; d) F. Schwer, S. Zank, M. Freiberger, R. Kaur, S. Frühwald, C. C. Robertson, A. Görling, T. Drewello, D. M. Guldi, M. von Delius, *Organic Materials* **2022**, *4*, 7-17.

[25] a) D. Ajami, J. Rebek, Jr., *J. Am. Chem. Soc.* **2006**, *128*, 15038-15039; b) D. Ajami, J. Rebek, Jr., *Nat. Chem.* **2009**, *1*, 87-90; c) F. U. Rahman, R. Wang, H. B. Zhang, O. Brea, F. Himo, J. Rebek Jr, Y. Yu, *Angew. Chem. Int. Ed.* **2022**, *61*, e202205534.

[26] a) H. D. F. Winkler, E. V. Dzyuba, C. A. Schalley, *New J. Chem.* **2011**, *35*, 529-541; b) K. D. Rand, S. D. Pringle, J. P. Murphy, K. E. Fadgen, J. Brown, J. R. Engen, *Anal. Chem.* **2009**, *81*, 10019-10028; c) M. E. Hemling, J. J. Conboy, M. F. Bean, M. Mentzer, S. A. Carr, *J. Am. Soc. Mass Spectrom.* **1994**, *5*, 434-442; d) M. A. Freitas, C. L. Hendrickson, M. R. Emmett, A. G. Marschall, *Int. J. Mass Spectrom.* **1999**, *185/186/187*, 565-575.

[27] H. D. F. Winkler, E. V. Dzyuba, J. A. W. Sklorz, N. K. Beyeh, K. Rissanen, C. A. Schalley, *Chem. Sci.* **2011**, *2*, 615-624.

[28] a) A. B. Kanu, P. Dwivedi, M. Tam, L. Matz, H. H. Hill, *J. Mass Spectrom.* **2008**, *43*, 1-22; b) F. Lanucara, S. W. Holman, C. J. Gray, C. E. Eyers, *Nature chemistry* **2014**, *6*, 281-294.

[29] a) E. Kalenius, M. Groessl, K. Rissanen, *Nat. Rev. Chem.* **2019**, *3*, 4-14; b) A. Kruve, K. Caprice, R. Lavendomme, J. M. Wollschläger, S. Schoder, H. V. Schröder, J. R. Nitschke, F. B. Cougnon, C. A. Schalley, *Angew. Chem. Int. Ed.* **2019**, *58*, 11324-11328; c) E. Hanozin, B. Mignolet, J. Martens, G. Berden, D. Sluysmans, A. S. Duwez, J. F. Stoddart, G. Eppe, J. Oomens, E. De Pauw, D. Morsa, *Angew. Chem. Int. Ed.* **2021**, *60*, 10049-10055; d) S. Ibáñez, C. Vicent, E. Peris, *Angew. Chem. Int. Ed.* **2022**, *61*, e202112513; e) C.-W. Chu, D. L. Stares, C. A. Schalley, *Chem. Commun.* **2021**, *57*, 12317-12320; f) M. C. Pfrunder, D. L. Marshall, B. L. Poad, T. M. Fulloon, J. K. Clegg, S. J. Blanksby, J. C. McMurtrie, K. M. Mullen, *Angewandte Chemie* **2023**, e202302229.

[30] a) R. Sure, S. Grimme, *J. Comput. Chem.* **2013**, *34*, 1672-1685; b) F. Neese, *WIREs: Comput. Mol. Sci.* **2012**, *2*, 73-78; c) F. Neese, *WIREs: Comput. Mol. Sci.* **2022**, *12*, e1606.

[31] a) S. Grimme, S. Ehrlich, L. Goerigk, *J. Comput. Chem.* **2011**, *32*, 1456-1465; b) V. K. Prasad, A. Otero-de-la-Roza, G. A. DiLabio, *J. Chem. Theory Comput.* **2022**, *18*, 2208-2232; c) R. Sure, S. Grimme, *J. Chem. Theory Comput.* **2015**, *11*, 3785-3801; d) J. G. Brandenburg, M. Hochheim, T. Bredow, S. Grimme, *J. Phys. Chem. Lett* **2014**, *5*, 4275-4284; e) M. Bursch, J.-M. Mewes, A. Hansen, S. Grimme, *Angew. Chem. Int. Ed.* **2022**, *61*, e202205735.

[32] U. Warzok, M. Marianski, W. Hoffmann, L. Turunen, K. Rissanen, K. Pagel, C. A. Schalley, *Chem. Sci.* **2018**, *9*, 8343-8351.

[33] a) M. Grajda, M. Wierzbicki, P. Cmoch, A. Szumna, *J. Org. Chem.* **2013**, *78*, 11597-11601; b) F. Jia, Z. He, L.-P. Yang, Z.-S. Pan, M. Yi, R.-W. Jiang, W. Jiang, *Chem. Sci.* **2015**, *6*, 6731-6738; c) Z. He, G. Ye, W. Jiang, *Chem. Eur. J.* **2015**, *21*, 3005-3012; d) M. Gaedke, H. Hupatz, F. Witte, S. M. Rupf, C. Douglas, H. V. Schröder, L. Fischer, M. Malischewski, B. Paulus, C. A. Schalley, *Org. Chem. Front.* **2022**, *9*, 64-74; e) P. Mal, B. Breiner, K. Rissanen, J. R. Nitschke, *Science* **2009**, *324*, 1697-1699; f) A. Shivanyuk, J. Rebek, Jr., *Proc. Natl. Acad. Sci. USA* **2001**, *98*, 7662-7665; g) A. Scarso, L. Trembleau, J. Rebek, Jr., *Angew. Chem. Int. Ed.* **2003**, *42*, 5499-5502; h) M. F. Bush, Z. Hall, K. Giles, J. Hoyes, C. V. Robinson, B. T. Ruotolo, *Anal. Chem.* **2010**, *82*, 9557-9565; i) V. Shrivastav, M. Nahin, C. J. Hogan, C. Larriba-Andaluz, *J. Am. Soc. Mass Spectrom.* **2017**, *28*, 1540-1551; j) D. P. Weimann, H. D. F. Winkler, J. A. Falenski, B. Koksch, C. A. Schalley, *Nat. Chem.* **2009**, *1*, 573-577; k) K. M. Ervin, P. B. Armentrout, *J. Chem. Phys.* **1985**, *83*, 166-189.

Entry for the Table of Contents

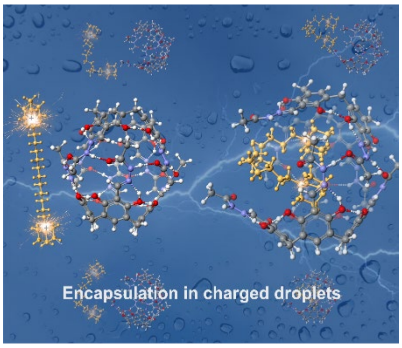

“Spring-loaded” resorcinarene capsules form in charged droplets: The complexes are not observed in solution and form during electrospray ionisation under conditions violating electroneutrality. The strained resorcinarene and dicationic guest complexes survive in the gas-phase due to strengthening of non-covalent bonds in the gas-phase enabling structural assignment via different tandem mass spectrometry techniques.

Institute and/or researcher Twitter usernames: @DanielStares @AgSchalley @fubcp